Journal of Biomedical Optics

SPIEDigitalLibrary.org/jbo

Spectroscopic imaging of serum proteins using quantum cascade lasers

Anadi Mukherjee
Quentin Bylund
Manu Prasanna
Yotam Margalit
Tarik Tihan

SPIE

Spectroscopic imaging of serum proteins using quantum cascade lasers

Anadi Mukherjee,[a] Quentin Bylund,[a] Manu Prasanna,[a] Yotam Margalit,[a] and Tarik Tihan[a,b]
[a]Infrasign LLC, 1440 Stone Pine Terrace #118, Fremont, California 94536
[b]University of California, Department of Pathology, Neuropathology Unit, 505 Parnassus Ave, San Francisco, California 94143

Abstract. First measurements of biomedical imaging using quantum cascade lasers (QCL) are presented. We report spectroscopic imaging of serum proteins using QCLs as an example for monitoring surface biocontamination. We found that dry smears of human serum can be spectroscopically imaged, identified, and quantified with high sensitivity and specificity. The core parts of the imaging platform consist of optically multiplexing three QCLs and an uncooled microbolometer camera. We show imaging of human serum proteins at 6.1, 9.25, and 9.5 μm QCLs with high sensitivity and specificity. The sensitivity limit of 3 $\mu g/cm^2$ of the human serum spot was measured at an S/N = 3.The specificity of human serum detection was measured at 99% probability at a threshold of 77 $\mu g/cm^2$. We anticipate our imaging technique to be a starting point for more sophisticated biomolecular diagnostic applications. [DOI: 10.1117/1.JBO.18.3.036011]

Keywords: quantum cascade lasers; biomedical; imaging; spectroscopy; biocontamination; serum.

Paper 130026LR received Jan. 17, 2013; revised manuscript received Feb. 15, 2013; accepted for publication Feb. 28, 2013; published online Mar. 20, 2013; corrected Mar. 22, 2013.

1 Introduction

Surface biocontamination is a major public health hazard that results in contaminated foods, drugs, cross-contamination of diseases in clinics/hospitals and public places such as restaurants.[1] An image-based device for full-surface screening of biocontamination can assure higher-quality healthcare for our citizens. Trace detection techniques such as mass spectrometry,[2,3] Fourier transform infrared spectroscopy (FTIR),[4] and chromatography[5] require swabbing a small sample area for testing. Although sensitive, these procedures are time-consuming, expensive, and do not cover 100% of the area that needs to be monitored regularly. To reduce public health hazards due to surface biocontamination significantly, a portable imaging system is needed that can detect, identify, quantify, and map out surface biocontamination on any amount of surface area with high sensitivity and specificity. Laser-based chemical imaging techniques explored so far are Raman[6] and near-infrared (NIR)[7,8] scattering. Fundamental absorption cross-section ($\sim 10^{-17}$ cm^2 mol^{-1}) > overtone absorption cross-section ($< 10^{19}$ cm^2 mol^{-1}) > Raman scattering cross-section ($\sim 10^{-29}$ cm^2 mol^{-1}).[9,10] Here we show that an efficient tag-less biomolecular imaging device can be made out of midwavelength infrared (MIR) lasers called quantum cascade lasers (QCL) and long wavelength infrared (LWIR) uncooled microbolometer cameras. We found that dry smears of human serum can be spectroscopically imaged, identified, and quantified with high sensitivity and specificity. We anticipate our imaging technique to be a starting point for more sophisticated biomolecular diagnostic applications.

2 Methods, Results and Discussion

When a MIR laser beam is tuned to an absorption peak of biomolecules of interest (e.g., Amide I peak of proteins), the beam is absorbed, and the scattered image will appear dark. A three-dimensional (3-D) stack of MIR images at different wavelengths (spectral hypercube) contains the entire biomolecular signature needed for diagnosis. Molecular recognition is most sensitive and selective at the absorption peaks. Images at the strongest absorption peak will be used for sensitivity measurement, and images at other wavelengths will be used to quantify specificity of detection via receiver operation characteristic (ROC) curves. Here we show the results of identifying human serum at a distance of 50 cm using our compact MIR imaging spectroscopy (MIRIS) setup.

Figure 1(a) shows the MIR imaging device with optically multiplexed 3 QCLs and a microbolometer camera. The home-built software operates the lasers, acquire and process images. Figure 1(b) shows the device details with three multiplexed QCLs, camera, digital to analog converter (DAC) board, and other optoelectronics. Image-based detection of explosives in the MIR have been reported via optothermal[10,11] and MIRIS[12,13] techniques. Optically multiplexed QCLs as reported here, are preferred to one broadly tunable[10–13] QCL because of wider frequency bandwidth availability (>3000 cm^{-1}) with higher optical powers. The three QCLs (6.1, 9.25, and 9.5 μm) were multiplexed[14] using a Galvo-mirror from Cambridge Technologies. The multiplexed beam was expanded to ~1.5 cm diameter on an aluminum plate 50 cm away from the device. The QCLs at were DFB devices while the QCL at 6.1 μm was a FP (Fabry-Perot) device. The QCLs obtained from www.atoptics.com were thermally cooled at 17°C. A DAC board and Linux OS were used for full device control.

Figure 2(a) shows the dried spot of random human serum on a CaF_2 slide. The serum spot is invisible when illuminated by visible light. The outline of the QCL beams is shown. Dried serum smears were produced by using a hole punched onto nonabsorbing tape as a mask for pattern transfer. 5 μl of serum was smeared onto the hole of the tape and dried. The

Address all correspondence to: Anadi Mukherjee, Infrasign LLC, 1440 Stone Pine Terrace #118, Fremont, California 94536. Tel: (510) 815 3365; E-mail: anadi@infrasign.com

0091-3286/2013/$25.00

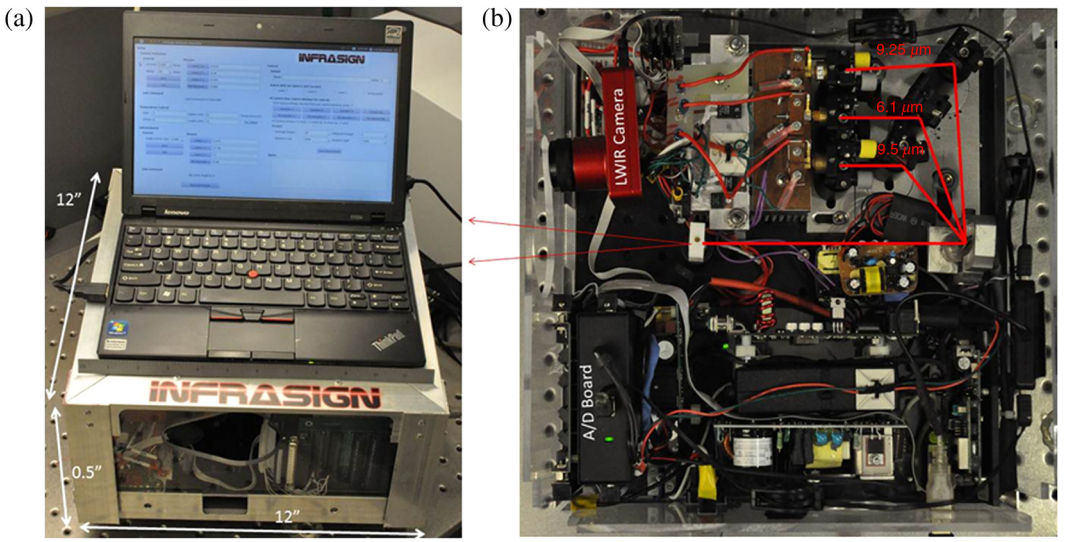

Fig. 1 Quantum cascade lasers (QCL) based MIR imaging system: (a) the device for QCL-based spectroscopic biomedical imaging. The software operate lasers, acquire and process images, (b) detail of the imaging device showing optically multiplexed three QCLs at wavelengths 9.25, 9.5, and 6.1 μm camera etc.

tape was then removed, leaving behind the dried serum spot on the slide. This way, dried serum smears with repeatable dimensions were produced. Diffuse scattering at each QCL frequency from the aluminum plate placed behind the slide were recorded by the microbolometer camera obtained from www.infraredcamerasinc.com.

Figure 2(b) shows the absorbance of the serum spot in 3-D when exposed to 6.1 μm QCL beam. The incident beam intensity normalized serum protein signal show strong sensitivity achievable in MIRIS based detection. This 3-D representation of absorbance of serum smear at 6.1 μm is shown in transmission (scatter from aluminum plate behind sample) in Fig. 2(c). The aluminum plate (5×10 in) used in the measurements was purchased off the shelf from a local hardware store and had no polish, only matte finish. Figure 2(c) also shows FTIR spectrum of the human serum recorded by

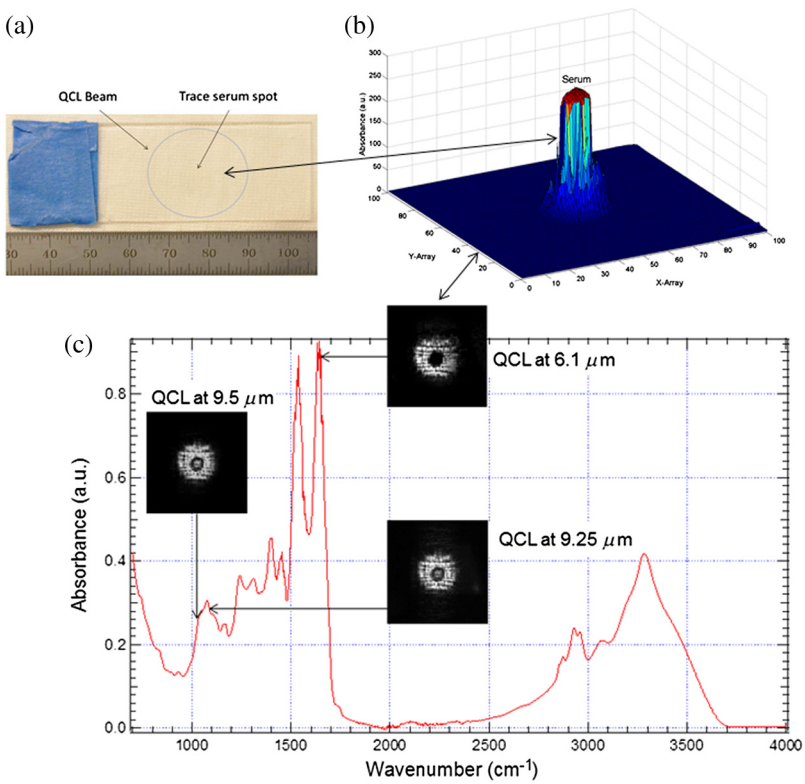

Fig. 2 Spectroscopic image detection of human serum on CaF_2 slide: (a) shows almost invisible serum spot on CaF_2 slide and the outline of illuminating QCL laser beam; (b) absorbance of the serum spot at 6.1 μm in 3-D corresponding to dark spot in shown in (c), FTIR spectrum recorded on the human serum and background subtracted MIR images of the serum spot taken by the camera under three QCL illumination at 9.5 μm (1052 cm^{-1}), 9.25 μm (1081 cm^{-1}), and 6.1 μm (1639 cm^{-1}).

Shimadzu IRAffinity-1 ATR-FTIR spectrometer. The FTIR data was stored after averaging over 40 spectra, with 4 cm^{-1} resolution and Happ-Genzel apodization. Three QCLs (6.1, 9.25, and 9.5 μm) are marked by arrows on the FTIR spectrum. The QCL at 6.1 μm (1639 cm^{-1}) being close to the Amide-I peak of proteins was chosen for high sensitivity protein imaging. The other two QCLs at 9.25 μm (1081 cm^{-1}) and 9.5 μm (1053 cm^{-1}) were around the glucose peak of the serum. Colinear QCL beams of CW power ~11 mW of each beam were turned on one at a time for illuminating the sample area on CaF_2 slide. The background-subtracted images of the dried serum spot at each laser wavelength are shown. The dried serum spot on CaF_2 slide that was invisible to visible light was clearly visible when illuminated by the 6.1 μm QCL beam. The serum spot looks dark due to the strong absorption of 6.1 μm QCL beam by Amide-I proteins while partial transparency (reduced absorption) is seen at the Glucose wavelengths (QCLs at 9.25 and 9.5 μm) as expected from the FTIR spectrum of serum. We see a good correspondence between the absorption values of FTIR spectrum with that of the pixel values of the recorded MIR images at the three QCL frequencies. The absorption ratio of Amide-I/Glucose ~3.12 in FTIR spectrum is close to the value ~3.2 measured in the central pixel values of the serum spot images. The dark annular ring of the serum spot at the Glucose wavelengths is due to thicker film at the edges than at the central region. We have studied 10 different human serum samples using MIRIS technique and all of them show the same behavior as the random one shown in this report. We found a standard error of ~5% around the signal-to-noise ratio of the random sample result shown in Fig. 2(c). The fringe pattern seen on the images are due to interference of QCL beams from the front and back surfaces of the slide. These fringe patterns are expected to be different on different surface materials on which the smear may be found (e.g., if the smear was directly on the aluminum plate, the fringes due to thin film effect of the smear and laser speckle patterns would influence the limit of detection). Surface quality of the substrate will also play a role in the diffuse scattering signal.[12,13] Laser despeckling can be used to get rid of these fringes and laser speckle that increase limit of detection[13] and reduce spatial resolution of imaging.

Figure 3 shows sensitivity of MIR image-based serum protein detection. Figure 3(a) shows the scatter image of 6.1 μm QCL beam (no serum) tuned to Amide-I protein peak. This beam profile was incident on dried serum smears at different dilutions to test the limit-of-detection (LOD) of our imaging system. Interference fringes seen on the incident beam is due to front and back surface reflections on the CaF_2 slide, and this was the source of most of the noise. The images shown was averaged over 1 s (i.e., 50 frames of the camera and the power stability of the lasers were <2%). The CaF_2 slides were polished on both sides by the manufacturer, which turned out to have a narrow wedge angle resulting in the interference fringes observed. The fringes are correlated to the 2-mm slide thickness and refractive index changes of CaF_2 at the QCL wavelengths due to normal dispersion. The refractive index of at 9 μm is 1.324, and at 6 μm is 1.383, and hence we see slightly narrower fringes at the shorter wavelength images. Figure 3(b) show the sequence of scatter images of the QCL beam at 6.1 μm for different serum dilutions starting with pure serum of 403 $\mu g/cm^2$ surface density. The surface density measurements shown in Fig. 3 included all solid biomolecular components in human serum, not just proteins (i.e., it includes proteins, nucleic acids, phospholipids, sugars, membrane lipids, fatty acids etc.,). Average protein content in human serum is ~70 g/L. For 5 μL of pure serum, we can expect around 350 μg of total proteins (Amide I, II, and II) in the measured 403 $\mu g/cm^2$ containing all biomolecular components in human serum. Since the QCL at 6.1 μm was tuned to Amide I peak, we were measuring dominantly Amide I, some Amide II, and a little of Amide III proteins due to absorption tails at this QCL wavelength. At each step of dilution, an equal volume of phosphate buffer was added to the last serum sample and dried in identical manner. No image

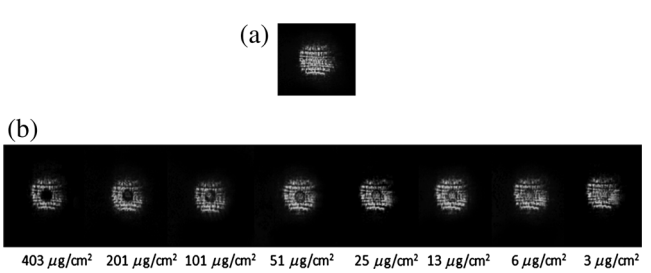

Fig. 3 Sensitivity of MIR image detection of human serum: (a) image of 6.1 μm QCL beam scattered off the aluminum plate placed behind the CaF_2 slide with no serum smear; (b) background subtracted MIRIS images of serum and diluted serums on CaF_2 slide taken near the Amide I peak of 6.1 μm (1639 cm^{-1}). The images of pure (403 $\mu g/cm^2$) and diluted serums show the decrease of contrast with diluted serum spots. The LOD of 3 $\mu g/cm^2$ was achieved without the use of laser despeckling or advanced image processing.

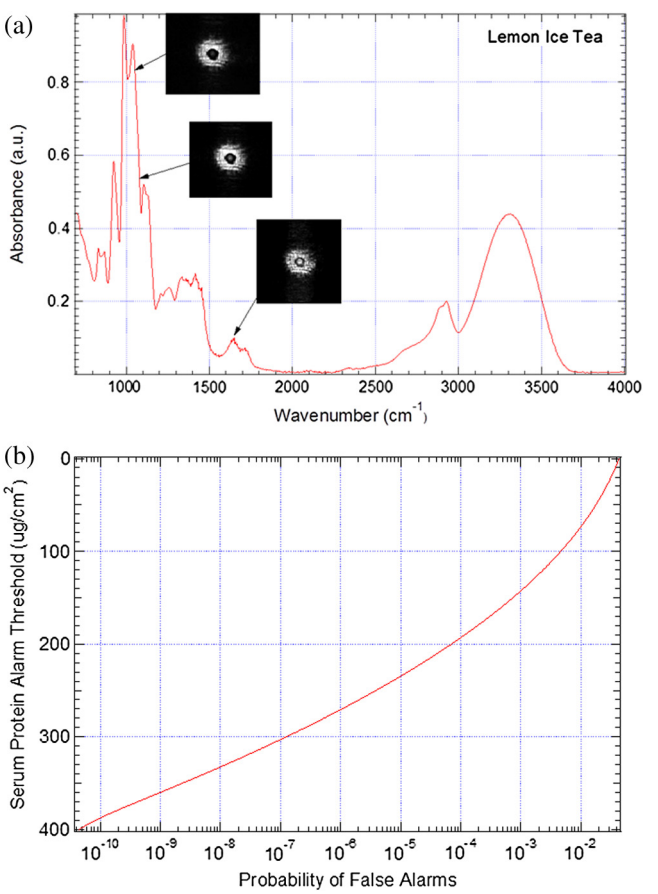

Fig. 4 Specificity of image detection of human serum: (a) lemon ice tea as a serum look-alike target; (b) ROC curve demonstrating PFA of 10^{-2} (PD of 99%) of human serum detection at a threshold of 77 $\mu g/cm^2$.

processing was used other than background subtraction. The decrease of contrast on serum detection versus decrease of surface density due to dilution of serum can be clearly seen. At the lowest total surface density of 3 $\mu g/cm^2$, the serum spot was still visible with an average $S/N = 3$. Considering the fact that we were actually sensing only proteins out of all biomolecular components in the total surface density, our measured LOD of 3 $\mu g/cm^2$ was a conservative estimate of total proteins in human serum. To the best of our knowledge, this is the lowest limit of detection reported so far[13] in any noninvasive image-based molecular recognition system. With despeckled laser beams and advanced image-processing techniques, we anticipate achieving an LOD of several 100 s of ng/cm^2. Such high sensitivity in image-based detection of biomolecules may perhaps enable quantitative stain-free pathology in the future.

Figure 4 shows the specificity of MIR image-based serum protein detection. Dried spots of serum look-alikes on the same slide (CaF_2) are indistinguishable under visible light illumination. Figure 4(a) shows MIR image of lemon ice tea that looks like serum in visible light but is clearly distinguishable using proper choice of QCL lasers. Also, serum protein may be found in myriads of surfaces that may have absorptions in the protein region. Such interferent rejection can be done following gas detection[15] using QCLs. Specificity is quantified as probability of detection (PD) or false alarm rates probability of false alarm (PFA) from ROC curve. The ROC curve calculations from our serum protein measurements on blank CaF_2 slide is shown in Fig. 4 following procedure reported in QCL based gas detection.[15]

3 Conclusion

As a simple demonstration of the first biomedical imaging using quantum-cascade lasers, we spectroscopically imaged trace amounts of human serum with high sensitivity and specificity. Using an optically multiplexed platform of three quantum cascade lasers and a microbolometer camera, we detected trace amounts of proteins in human serum as low as 3 $\mu g/cm^2$. High specificity of protein detection in human serum was demonstrated by the spectroscopic images of lemon ice tea taken as an example of a serum look-alike substance. Specificity was quantified via ROC curve showing PFA of 10^{-2} (99% PD) for human serum detection at a threshold of 77 $\mu g/cm^2$. By a proper choice of QCL wavelengths and/or multiplexing more lasers, we would be able to distinguish between different biomaterial sources containing proteins. This image-based biocontamination sensor can be applied in the areas of security from biohazards, food safety, cross contamination in clinical ambiance, etc. It is also a preliminary example showing the potential of MIRIS-based technology toward most advanced label-free, noninvasive medical diagnostic applications that are well known in the biomedical industry.

Acknowledgments

We gratefully acknowledge laboratory support and associated help from Department of Pathology, UCSF; help we received from Mariano Troccoli of Adtech Optics regarding QCLs, Gary Strahan of Infrared Cameras Inc., regarding microbolometer camera and many helpful discussions with Biswaroop Mukherjee throughout the course of this project.

References

1. "Cleanrooms and associated controlled environments—biocontamination control—Part 2: Evaluation and Interpretation of Biocontamination data," document No. ISO 14698-2, DIN EN ISO 14698-2, 4th edn., http://www.ihs.com (2010).
2. P. P. Hurtado and P. B. O'Connor, "Differentiation of isometric amino acid residues in proteins and peptides using mass spectrometry," *Mass Spectrom. Rev.* **31**(6), 609–625 (2012).
3. M. Bantscheff et al., "Quantitative mass spectrometry in proteomics: a critical review," *Anal. Bioanal. Chem.* **389**(4), 1017–1031 (2007).
4. A. Barth, "The infrared absorption of amino acid side chains," *Rev. Prog. Biophys. Mol. Biol.* **74**(3–5), 141–173 (2000).
5. B. Shushan, "A review of clinical diagnostic applications of liquid chromatography-tandem mass spectrometry," *Mass Spectrom. Rev.* **29**(6), 930–944 (2010).
6. B. Shushan, "Label-free imaging of biomolecules in food products using Raman microscopy," *J. Biomed. Opt.* **16**(2), 021118 (2011).
7. U. Mahmood, "Near infrared optical applications in molecular imaging," *IEEE Eng. Med. Bio.* **23**(4), 58–66 (2004).
8. G. Reich, "Near-infrared spectroscopy and imaging: basic principles and pharmaceutical applications," *Adv. Drug Deliv. Rev.* **57**(8), 1109–1143 (2005).
9. W. Demtroder, "Laser spectroscopy: basic concepts and instrumentation," in *Springer Series in Chemical Physics*, F. P. Schafer, Ed., Vol. 5, Springer-Verlag, Berlin Heidelberg (1982).
10. A. Mukherjee et al., "Standoff detection of explosive substances at distances up to 150 meters," *Appl. Opt.* **49**(11), 2072–2078 (2010).
11. C. A. Kendziora et al., "Infrared photothermal imaging for standoff detection applications," *Proc. SPIE* **8373**, 83732H (2012).
12. B. E. Bernacki and M. C. Phillips, "Standoff hyperspectral imaging of explosives residues using broadly tunable external cavity quantum cascade laser illumination," *Proc. SPIE* **7665**, 766501 (2010).
13. F. Fuchs et al., "Imaging standoff detection of explosives using widely tunable midinfrared quantum cascade lasers," *Opt. Eng.* **49**(11), 111127 (2010).
14. A. Mukherjee et al., "Optically multiplexed multi-gas detection using quantum cascade laser photoacoustic spectroscopy," *Appl. Opt.* **47**(27), 4884–4887 (2008).
15. A. Mukherjee et al., "Sub-parts-per-billion level detection of dimethyl methyl phosphonate (DMMP) by quantum cascade laser photoacoustic spectroscopy," *Appl. Opt.* **47**(10), 1543–1448 (2008).